

The Autoregressive Analysis for Wind Turbine signal postprocessing

Daniel Pereiro, Ikerlan, Felix Martinez, Ikerlan, Iker Urresti, Ikerlan, and Ana Gómez González, USC,

Abstract—Today modern simulations solutions in the wind turbine industry have achieved a high degree of complexity and detail in result. Limitations exist when it is time to validate model results against measurements. Regarding Model validation it is of special interest to identify mode frequencies and to differentiate them from the different excitations. A wind turbine is a complex device and measurements regarding any part of the assembly show a lot of noise. Input excitations are difficult or even impossible to measure due to the stochastic nature of the environment. Traditional techniques for frequency analysis or features extraction are widely used to analyze wind turbine sensor signals, but have several limitations specially attending to non stationary signals (Events). A new technique based on autoregressive analysis techniques is introduced here for a specific application, a comparison and examples related to different events in the wind turbine operations are presented.

Keywords—wind turbine, signal processing, mode extraction.

I. INTRODUCTION

SINCE the last decades wind energy has been growing in the power supply market becoming one of the fastest growing energy sources. To harvest energy from the wind the horizontal axis wind turbine is the more extended design. Due to the particular characteristics of this kind of power generation device, the output of a single machine increases with a quadratic relation with the wind turbine rotor diameter, the aim of bigger machines is clear, reaching today bigger ones more than 3 MW per turbine.

As machines increase size, loads get bigger and so natural frequencies decrease in frequency value. Proper design rules and simulation tools are required to reach regulations demands: design life for 20 years [1]. Older especifications and design techniques for the differents subassemblies do not match this booming market demands and correct design tools for bigger turbines becomes a challenge and a necessity [6].

Even regulations and rules related to wind turbines exist, new developments of new wind turbines relay more than ever in numerical calculations and computer simulations. Despite the models have achieved a high degree of complexity, from aero elastic, dynamics and power generation to the control. Confidence in the results they provide do not follow the intended use of the model. Having a more complex model does not mean that the obtained results are going to be better. The validity of these simulations has a very high dependence in the correct estimation of the inputs parameter values used in models. A clear example of this complexity is the gearbox modeling. There are available a great number of models to

simulate the internal behavior but it is still common practice to simplify this component by a single degree of freedom torsion spring.

Even if during the construction of the prototype some component validations are done, once the prototype is built the main task is to verify if the real behavior relays close to the predictions obtained with the models. The global wind turbine validation is normally carried out by comparing in the frequency domain the results of accelerometers and sensors placed in the prototype with the same data provided by the simulations. The first objective is to identify tower and blades frequencies that normally are in the same range of operational excitations as low speed shaft rotational speed.

In order to identify modes and excitations the most common graphic representation is a waterfall PSD and campbell diagrams [5] for rotordynamics. Waterfalls are calculated where the abscissa axis normally correspond to the frequency and the ordinate axis to the mean wind speed or even power output while in campbell diagrams abscissa axis correspond to the frequency and ordinate to angular speed of the different parts. Stable peaks at different wind speed levels shows the frequency values of the wind turbine modes, this technique focus on mode excitations for the different wind speed condition while some mode or excitations are neglected. Even this kind of graphical representation is usefull it does not allow the analyst to study events or operations of the wind turbine where frequency content only appear during a short period of time.

The used techniques are normally based in Fourier transform analysis as it can be seen for example in [7]. FFT based techniques have several limitations first, and maybe the most important is that it supposes stationary nature of the signal object of study, so for transition events and regarding the usually low sampling frequency and long measuring runs classical methodologies are limited.

A new approach to signal treatment in wind turbines sensing attending to frequency behavior of the system is presented in this article. Auto Regressive (AR) techniques are presented as an improvement from classical approaches as FFT. This new technique allows for the same time series to achieve higher accuracy on mode frequency identification, and also been able to correctly differentiate between excitations and modes.

The AR methodology is presented and compared against classical methods and then using real measurements both methodologies are applied to show differences.

II. AUTOREGRESSIVE METHOD (AR)

Fourier based analysis techniques have several limitations: the first one is that it assumes stationary nature of the time

series while in many dynamic systems and specially for transition events this is not true. Secondly it does not separate the effects of amplitude and phase from each other because the signals are decomposed into a sum of sinusoidal waves with constant amplitude. In windowed Fourier analysis for non-stationary signals each window still is not able to capture temporal informations despite the improvement [4].

On the contrary autoregressive techniques use parametric models. With this technique the signal is approximated by a linear difference equation with complex coefficients:

$$x[n] = u[n] - \sum_{k=1}^p a[k]x[n - k] \quad (1)$$

Where $x[n]$ is the output sequence of a filter (order p) and $u[n]$ is the conducting noise. With zero mean and variance σ_u^2 .

Regarding [3] the PSD of a signal with such structure is totally described in terms of model parameters through the equation.

$$\hat{P}_{AR(f)} = \frac{\sigma_u^2}{|1 + \sum_{k=1}^p a[k]e^{-i2\pi f k}|} \quad (2)$$

Once the signal has been approximated to the linear difference equation (modeled) the PSD obtained is analytical and directly calculated. There are no more needs for time average.

This improvement in frequency analysis came with the price of higher computational burden, so this has to be taken into account for setting window and overlap parameters. However, this limitation is not a major issue if single signals are to be analyzed.

As the scope of this paper is to outline the benefits of AR techniques over traditional techniques related to events, spectrograms are used. These representations allow the analyst to account for the frequency content during the event with higher spectral resolution.

One of the more important aspects when it is time to work with AR methodologies is the order used at each windowed time section. The spectral resolution achieved with AR techniques is directly related to the order of the filter (equation 2) used in the signal processing. According to [3] the order is automatically calculated for each window of the spectrogram.

If the order is set to be variable for each of the windowed time section, amplitude comparison is not possible along spectrogram because different orders result in different amplitude scale. To avoid this and to track modes and excitations in spectrograms, the order of the spectrogram is set to the maximum of all windowed time lapse.

To better illustrate the capabilities of the AR techniques a demonstration is previously presented using a test function.

$$A(t) = 2(1 - \cos(2\pi t/60))\sin(6\pi t) \quad (3)$$

$$B(t) = 6\sin(10\pi t) \quad (4)$$

$$C(t) = 5\sin(2\pi(0.5 + t/20) * t) \quad (5)$$

$$D(t) = \text{White Gaussian noise } 3\text{db} \quad (6)$$

$$\text{Test signal} = A + B + C + D \quad (7)$$

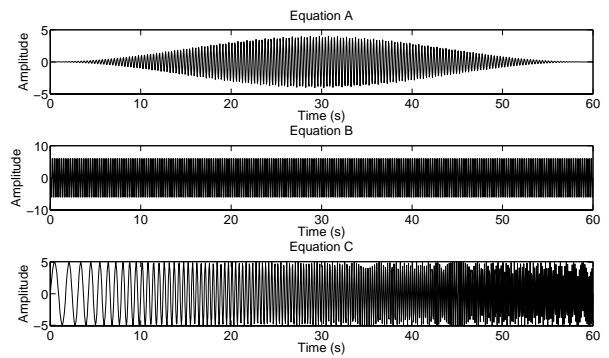


Fig. 1. Different sinusoidal components for the Test Signal

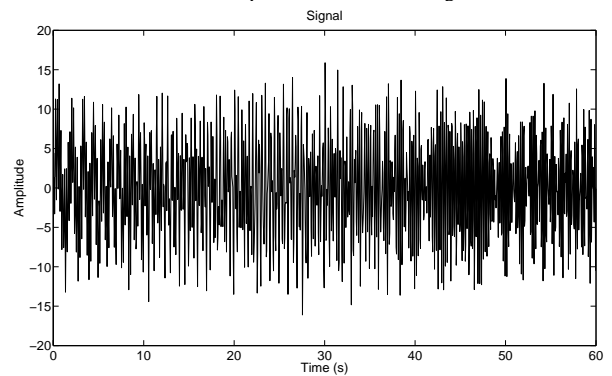


Fig. 2. Test Signal

In the test function (equation 7) constant sinus (equation 4), frequency varying sinus (equation 5), amplitude varying sinus (equation 3) and white noise (equation 6) are used with the aim of a more realistic illustration. For this Test function a sampling frequency of 20 Hz is used. The three different sinusoidal signals can be seen in Figure 1.

The final signal (equation 7) is plotted in Figure 2 and it is the result of the sum of the three different signals plus the white noise.

The test signal here presented is analyzed using AR techniques and classical methodologies as FFT based techniques, always following the method described in [3]. The calculation is set to a time window of 100 points and an overlap of 90 points. Both of them are analyzed with a peak stractor to better show the frequency content of the signal and to make a better comparasion. Spectrograms can be seen in Figures 3 and 4 respectively.

Attending to Figures 3 and 4 both of the techniques show the three components of the test signal but with the AR thechnique the frequency accuracy is higher.

A peak stractor is used to better appreciate the differences. The peaks can be seen in Figure 5 and Figure 6.

The difference according to the number of time windows is due to the fact that with FFT spectrograms an average is done attending to the blocks in wich the signal is divided. This is done to achieve the best possible frequency resolution for an

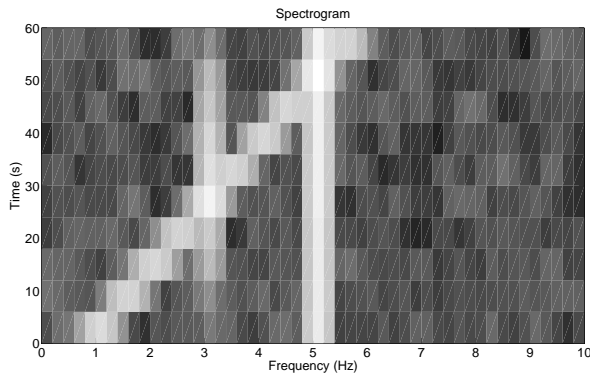


Fig. 3. Test Signal Spectrogram FFT

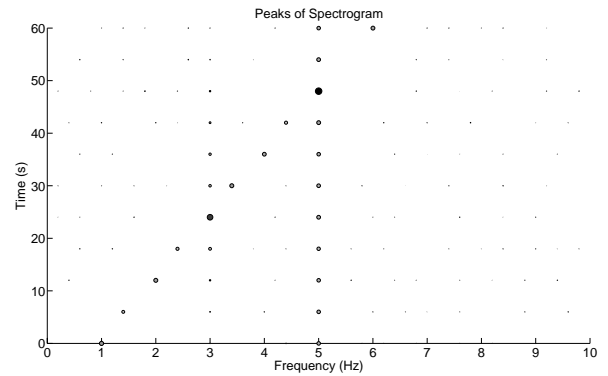


Fig. 5. Test Signal peaks FFT

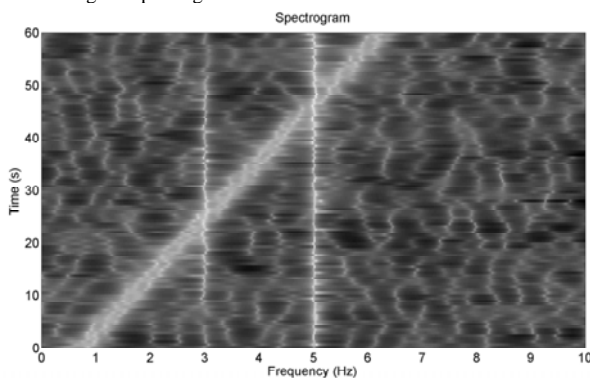


Fig. 4. Test Signal Spectrogram AR

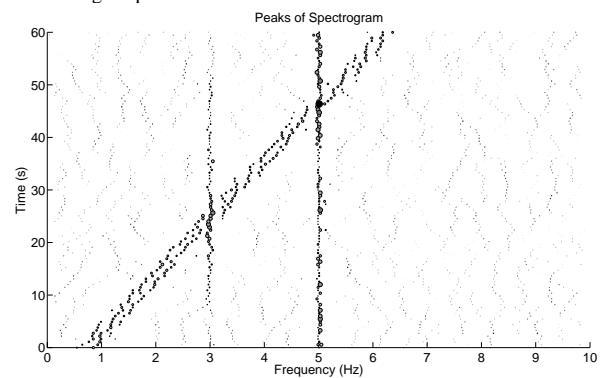


Fig. 6. Test Signal peaks AR

specific time discretization. There is no need for time average using AR method, so the improvement is not just restricted to the resultant frequency accuracy but also time accuracy for the spectrogram.

To illustrate this an spectrogram using FFT techniques with same overlap and window values is done. This spectrogram is shown in Figure 7. The frequency accuracy will be set in both cases Figure 3 and Figure 7 by the window and the sampling frequency for this case $f_r = 1/Period$ so being a 5s window and 20 Hz of sampling frequency: $f_r = 0.2 Hz$. As it can be seen the peaks now are narrower but there is no gain in frequency accuracy between Figure 7 and Figure 3. In further representation the FFT based spectrograms will be presented without the overlapped lines, an average will be done instead.

One thing that must be taken into account is that while FFT techniques are real results (with physical meaning both in amplitude and in frequency) with AR techniques the result is an approximation and as an approximation it is limited according to the physical meaning of the results that provide. It is true that with AR techniques the frequency content is correctly reflected in terms of the frequency value but not the amplitude. This is the reason why for the AR spectrogram peaks are not as equal as FFT peaks. The bigger inconvenience of using AR techniques will be so dealing with peak amplitudes, which can be compared along the spectrogram (Because the order of every window is fixed) but not between spectrograms from different signals.

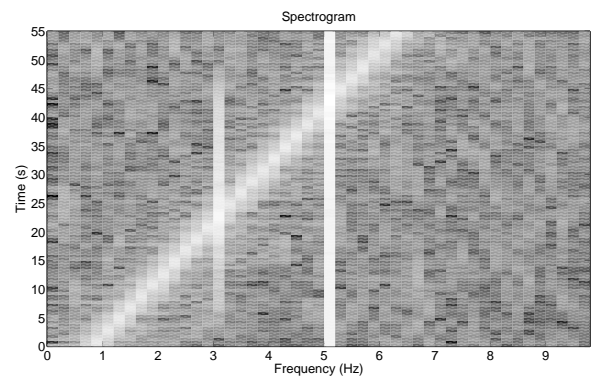


Fig. 7. Test Signal Spectrogram FFT with overlap

In the other hand what make AR techniques something of value is the accuracy gain as it is shown in Figures 5 and 6. Due to the fact that more and closer peaks can be observed using AR, now the analyst can follow fast frequency variations during an analyzed event or be able to see modes or excitations that can barely be detected with traditional techniques. In the next chapter real measurements will be analyzed and both techniques compared.

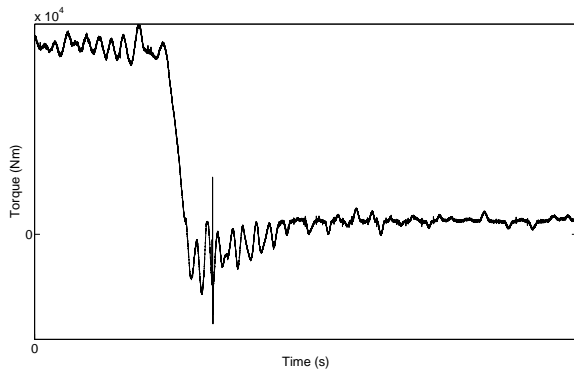


Fig. 8. Measured HSS torque signal. Emergency Stop

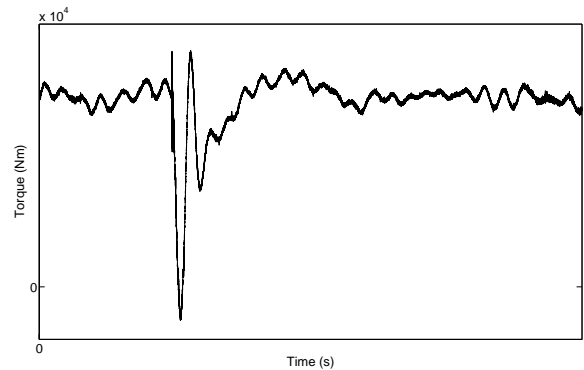


Fig. 9. Measured HSS torque signal. Power hole

III. EXPERIMENTAL SETUP

The signals used to illustrate this paper correspond to several measurement campaigns in a 3MW prototype from ALSTOM WIND installed in a test field near Tarragona (SPAIN).

The measurements campaigns where the signals are used for this analysis are part of wider scope campaigns to obtain global features for full models and for certification purposes. Some of the results regarding one of the campaigns were presented on IMAC2011 [2].

This are the signals used to outline the benefits of the AR technique for post processing data: Torque in the high speed shaft (twice) and accelerations of the gearbox. The latter are typical for mode extracting but for the scope of the paper torque signal will be also used in order to present AR techniques potential.

A. Emergency stop

The first signal extracted is a torque measurement on the High speed shaft (HSS) elastic coupling. For that purpose a dedicated optical sensor was placed in the elastic coupling. The event is recorded at a sampling frequency of 500 Hz for a 5 minutes run. Only 60 seconds of the time series, corresponding to an emergency stop are selected for this analysis. In Figure 8 the signal to be analyzed is shown.

Before the signal is analyzed in frequency content some preprocessing is required. Offset is extracted from the original signal and then a high pass filter (butterworth filter of order 4 and cut frequency of 0.3 Hz) and a resample to see only low frequencies.

The high pass filter only avoids high energy components of the signal at very low frequencies. In figure 8 can be seen that machine drops from nominal value to almost zero in little time. The Generator speed signal will be used as reference to plot speed related excitations over the spectrogram.

B. Power Hole

The signal is a torque signal related to a power hole triggered in the generator. The time series has a sampling frequency of 20000 Hz during one minute measurement. For this example only the first 40 seconds will be used.

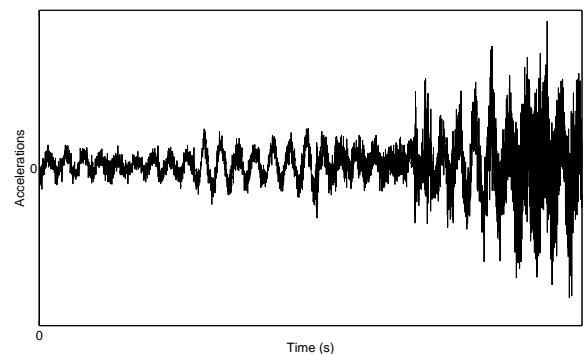


Fig. 10. Measured Gearbox lateral accelerations. Start up

In Figure 9 the signal follows a similar process to Figure 8 signal. The same preprocessing as in the previous signal is implemented (same filter with the same order and resample to achieve a 50 Hz limit). The speed signal would be used as reference to plot power train excitations over the spectrogram.

C. Start up

In this case the signal corresponds to the lateral accelerations of the gearbox. The event used for this example is related to start up operation for the machine under significant wind condition (20 m/s approximately). The sampling frequency is 100 Hz, low pass filter is applied to the original signal and offset is also extracted. For this example resample is applied to the signal to set spectrogram frequency limit in 25Hz.

The acceleration signal is presented in Figure 10, for this example 100s event is analyzed. Rotational speed is also used to plot excitations over the spectrogram.

IV. APPLICATION TO A CASE OF INTEREST

Results are presented using spectrograms, so x axis would be frequency and y axis will be time. Even if other representations are more common, such as with wind speed or electrical power on the y axis, representing the frequency response during time gives more informations about the transient content of the signal. This is one of the main advantages of not considering the signal as stationary, as FFT based

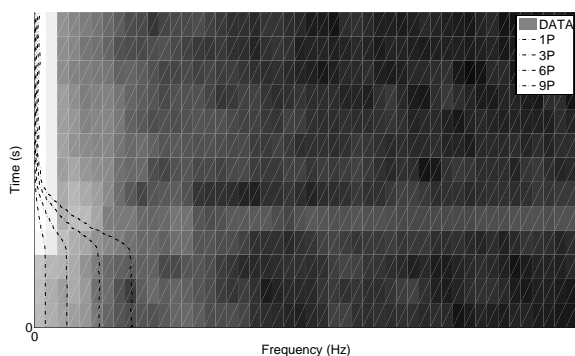


Fig. 11. Emergency Stop spectrogram FFT

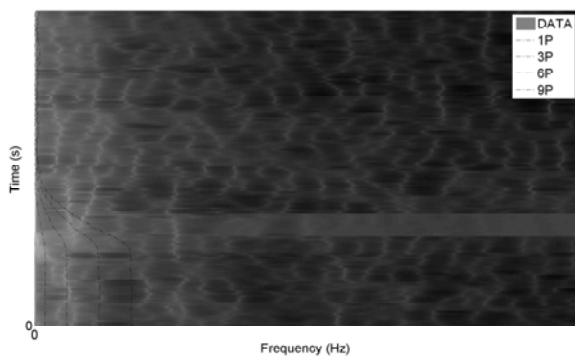


Fig. 12. Emergency Stop spectrogram AR

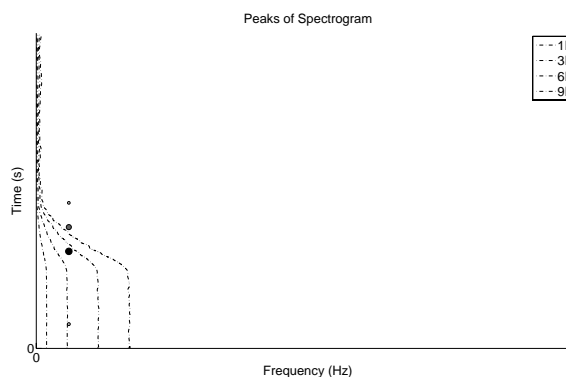


Fig. 13. Emergency stop spectrogram peaks FFT

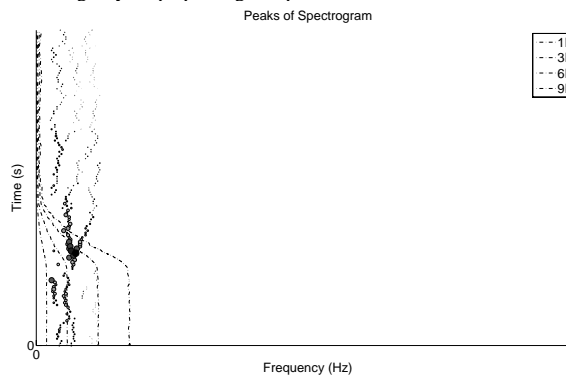


Fig. 14. Emergency stop spectrogram peaks AR

techniques does. Adding to the spectrogram rotational speed dependent excitations, gearbox, gear mesh and rotational speed of the different axes allows the analyst to correctly separate the excitations frequencies from the modes of the structure. It also helps to identify patterns in the analyzed signals, even if they are shifted in frequency. Along with the different spectrograms the result of the peak extraction is also presented to better illustrate the advantages of the technique here presented.

A. Emergency Stop

A grid loss event is when during normal operation of the wind turbine grid connection suddenly drops and resistive torque in the generator goes to zero. In consequence control reacts with an Emergency stop. The machine stops in seconds to prevent over speed resulting in the excitation of several components or subassemblies of the structure.

In Figures 11 and 12 the same signal spectrogram is calculated with AR techniques (Figure 12) and FFT techniques (Figure 11).

As it can be seen at the beginning of the test, 3P excitation is identified as it can be seen in Figure 12, but when the machine starts slowing down, the first drive train mode (slightly above 3P excitation) is not any longer identified in the FFT spectrogram while it can be observed in the AR spectrogram for several seconds (Figure 12) when the machine is almost stopped and while excitations pass over the frequency.

It can be also outlined from this representation that superimposing the speed of the different sources of excitations

makes the spectrogram analysis easier in order to differentiate between excitations and modes. It is even clearer in the peaks extracted from both spectrograms. Both results can be seen in Figures 13 and 14. Only frequency interval is plotted to highlight the commented peaks.

With the peak representation the difference is even clearer, while peaks extracted for FFT spectrogram only show two peaks in the region of interest in the peaks extracted for the spectrogram with AR techniques a series of peaks can be seen clearly proving the benefits of AR techniques and neglecting the source of such frequency excitation.

B. Power Hole

For this example another transition event is selected, in this case a power hole. This events consists of a short power drop that is triggered during normal machine operation. A power hole is a generator related issue. First appears a shortcut and then a sudden drop in the demanded torque for few seconds until generator control is enabled again. This lead to excitations and to a fast variation on the rotational speed of the system. For this example Generator rotational speed is plotted.

In Figures 15 and 16 the same signal spectrogram is calculated with AR techniques (Figure 15) and FFT techniques (Figure 16).

For this example similar peaks can be seen for both spectrograms (AR and FFT), but for autoregressive techniques

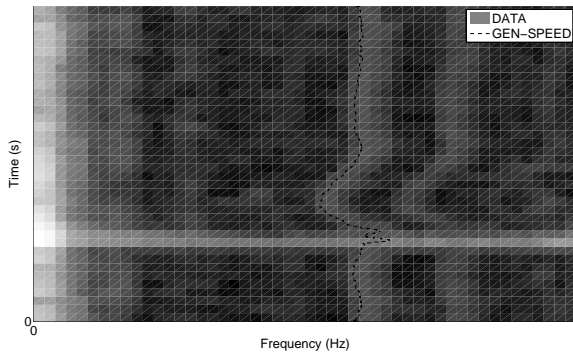


Fig. 15. Power Hole spectrogram FFT

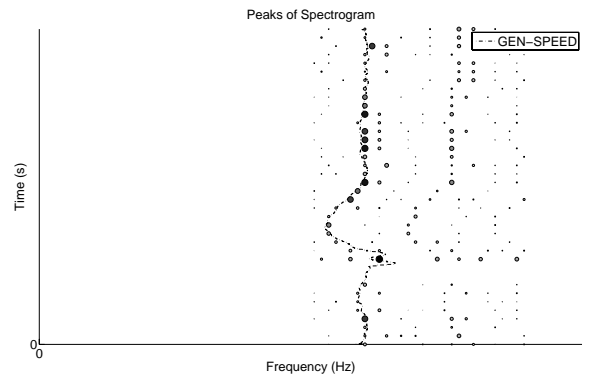


Fig. 17. Power Hole spectrogram peaks FFT

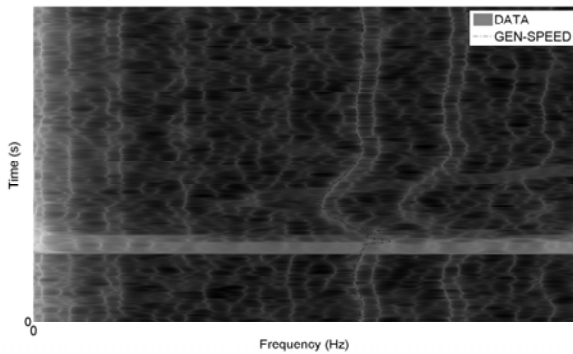


Fig. 16. Power Hole spectrogram AR

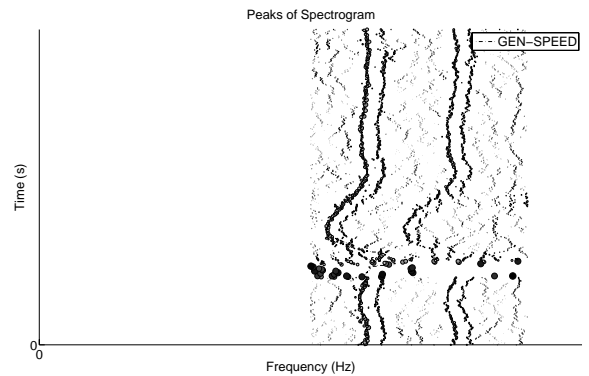


Fig. 18. Power Hole spectrogram peaks AR

the spectral resolution has a clear improvement. In AR spectrogram the excitation related to the Generator speed can be precisely identified. What is more peculiar is the other excitation that can be seen just besides the excitation (in higher frequency), this can be due a sort of sidebands effect.

In Figures 17 and 18 the peak extracted from spectrograms can be seen.

For AR techniques the peaks in Figure 18 follow with good accuracy the generator speed excitation. Once again for the peaks extraction a filtering was done.

C. Start up

For the last example an event where start up operation can be seen is selected. The lateral accelerations for the gearbox housing is selected as the signal to analyze. The spectrograms between both techniques for this example are presented in Figures 19 and 20.

For this example it can be noticed again that the frequency resolution shows a big improvement. While for classical techniques some modes or excitations are barely seen with AR techniques this kind of doubts can be answered. For example there are two lines that are almost constant in frequency while the machine is stopped and start moving during the start of the machine. This two lines can be confused with speed related excitations attending to FFT spectrogram but there is no more ambiguity attending the AR spectrograms. The difference is even clearer attending at the extracted peaks that can be seen in Figures 21 and 22

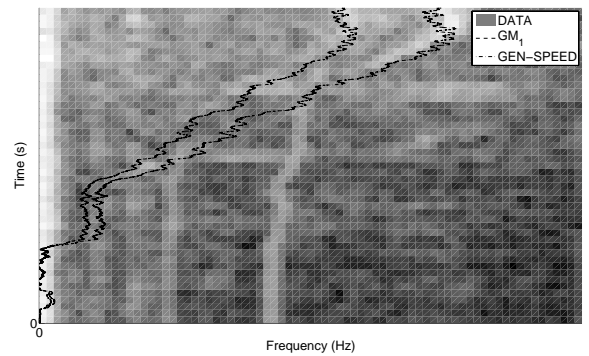


Fig. 19. Start up spectrogram FFT

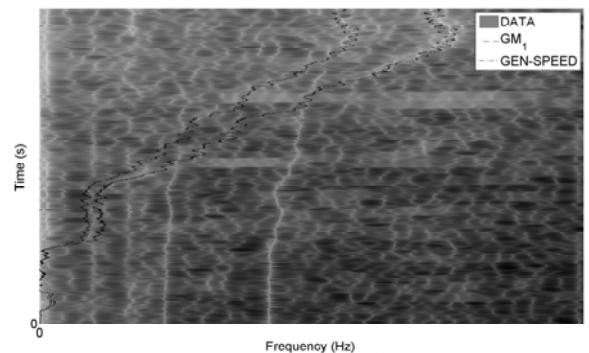


Fig. 20. Start up spectrogram AR

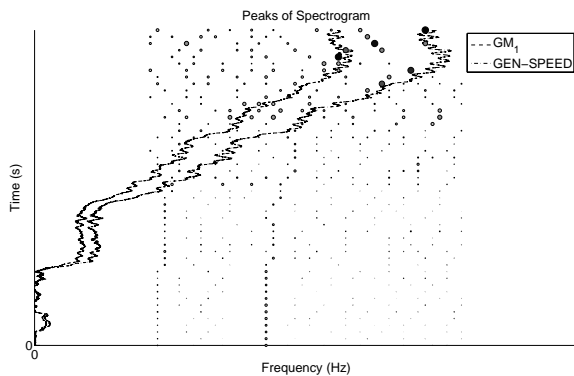


Fig. 21. Start up spectrogram peaks FFT

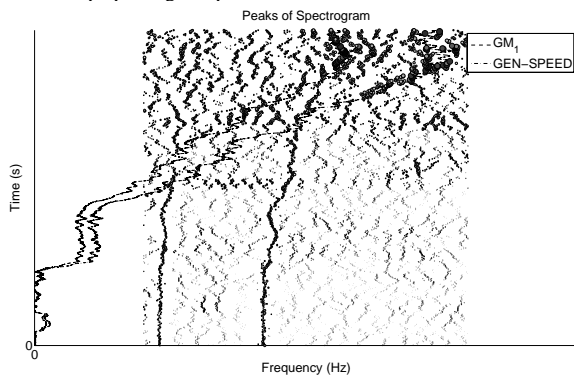


Fig. 22. Start up spectrogram peaks AR

For this peak extraction a filtering process was done because peaks and excitations increase significantly in amplitude once the machine starts running leading to noise. Another aspect that is highlighted in this analyzed event is the fact that with AR techniques excitations can be followed more precisely than for classical techniques as it was commented in Section IV-B.

V. CONCLUSIONS

Traditional techniques for data post processing exhibits some limitations to extract all the relevant data from the signal. This paper compares the results obtained from FFT and AR techniques showing that the latter allows obtaining smoother data, and hence, a more precise value of the peaks in frequency domain.

Another relevant aspect of the proposed analysis is to introduce the time variable to detect transitory events in the signal, which allows detecting frequencies that are excited only during a short period of time. AR techniques have been proved useful to identify mode excitations that comprises just a few cycles, with higher accuracy on frequency domain than classical solutions.

The detection of these transitory frequencies is a key point in model validation of complex systems as wind turbines. Excitations in many cases can hide the internal vibrations of the different subassemblies. The power train of a wind turbine is a clear example of this kind of problem as it is shown in the present paper for example in IV-A.

We would not be fair not to comment the disadvantages that exist attending to this kind of methodologies as it is the fact that peak amplitude extracted from AR techniques have a limited physical meaning. Setting the same order for each time step of the analyzed signal allows the analyzer to compare modes and excitations in one spectrogram but it is not possible to compare the different level of excitations attending to different spectrograms, different signals.

The aim of ongoing research projects related to this issue is to introduce such techniques in model validation activities like mode extraction.

REFERENCES

- [1] Iec 61400-1 wind turbines - part 1 design requirements.
- [2] J. Basurko, O. Salgado, I. Urresti, D. Tcherniak, S. Chauhan, A. Rodriguez-Tsouroukdissian, and C.E. Carcangiu. Test / model correlation in the alstom 3 megawatt wind turbine. In *IMAC XXIX, Jacksonville-FL, USA*, 2011.
- [3] A. Gómez González, J Rodríguez, X. Sagartzazu, A. Schumacher, and I. Isasa. Multiple coherence method in time domain for the analysis of the transmission paths of noise and vibrations with non stationary signals. In *Proceedings of ISMA 2010*, 2010.
- [4] Mahadevan. S Jiang. X. Wavelet spectrum analysis approach to model validation of dynamic systems. *Mechanical Systems and Signal Processing*, 25:575–590, 2011.
- [5] F. Vanhollebeke B. Marrant W. Meeusen J. Peeters, S. Goris. A need for advanced and validated multibody models as a basis for more accurate dynamic load prediction in multimegawatt wind turbine gearboxes. In *Proceedings of ISMA 2010*, 2008.
- [6] F. Oyague. Gearbox modeling and load simulation of a baseline 750-kw wind turbine using state-of-the-art simulation codes. Technical report, NREL/TP-500-41160, February 2009.
- [7] Y.M. Cho S.H. Ahn C.K. Song Z. Hameed, Y.S. Hong. Condition monitoring and fault detection of wind turbines and related algorithms: A review. *Renewable & Sustainable Energy Reviews*, 13:1–39, 2009.